

# Application of Binary Genetic Algorithm for Holographic Vascular Mimicking Phantom Reconstruction

Tugba Ozge Onur and Gulhan Ustabas Kaya

**Abstract**—Since medical imaging is one of the essential methods for the diagnosis and treatment of several diseases, the characterization and calibration of medical imaging systems with low-cost equipment is the most crucial issue. In this context, tissue-mimicking phantoms have long been used for this purpose. The advantage of phantoms is that, in addition to the desired size and internal properties, they can be produced in a way that best carries the characteristic properties of tissue models and can be standardized so that they can be used in imaging environments. For this reason, it is important to make low-cost phantom designs produced from materials that are easy to shape and available and to ensure that they can be imaged with high quality.

In this study, digital holography and binary genetic algorithm (BGA) were used to reconstruct the images of phantoms that mimic the human vascular system produced at a low cost. The obtained results showed that BGA can be used as an alternative to the reconstruction methods commonly used in digital holography. Since BGA provides an alternative solution to obtain the image with high resolution in the reconstruction process without any image processing algorithm, it enables the diagnosis of diseases related to thin vascular structures in real-time with a reliable and non-contact method.

**Index Terms**—binary genetic algorithm, lateral shearing, reconstruction, thin vessel structures, tissue-mimicking phantom.

## I. INTRODUCTION

PHANTOMS ARE artificial tissues that are used as an alternative to human tissue and that allow the diagnosis of disease to be made non-contact without taking samples from patients. Phantoms are used for many different purposes in the medical sense such as identification of cancerous cells or detection of tissue changes in organs, examination of vascular structures, and so on [1-3].

TUĞBA ÖZGE ONUR, is with Department of Electrical-Electronics Engineering, Zonguldak Bülent Ecevit University, Zonguldak, Turkey, (e-mail: [tozge.ozdinc@beun.edu.tr](mailto:tozge.ozdinc@beun.edu.tr)).

 <https://orcid.org/0000-0002-8736-2615>

GÜLHAN USTABAŞ KAYA, is with Department of Electrical-Electronics Engineering, Zonguldak Bülent Ecevit University, Zonguldak, Turkey, (e-mail: [gulhan.ustabas@beun.edu.tr](mailto:gulhan.ustabas@beun.edu.tr)).

 <https://orcid.org/0000-0002-5643-0531>

Manuscript received October 05, 2021; accepted Dec 21, 2021.  
DOI: [10.17694/bajece.1004981](https://doi.org/10.17694/bajece.1004981)

Phantoms are the test materials that can depict the special characteristics of human tissues in medical imaging applications. Tissue mimicking phantoms have been utilized to qualify and calibrate medical imaging systems for a long time. In addition, phantoms are utilized for comparing the performances of medical imaging systems, training technicians using these systems, and developing new imaging systems and devices. The advantage of phantoms is that, in addition to the desired size and internal properties, they can be produced in a way that best carries the characteristic properties of tissue models and can be standardized so that they can be used in imaging environments. For this reason, it is important to be able to create low-cost phantoms made of materials that are easy to make, shape, and find.

The structure of the produced phantoms differs from each other about the area in which they will be used. For this reason, the materials used in the preparation of the phantom also change. For instance, polyacrylamide (PAA), which has solid elastic and optically transparent properties, was produced with acrylamide C3H5NO and water by Singh *et al.* The temperature fluctuations do not change in PAA [4]. Agar gel is prepared with water-gel structure by changing the temperature. The bonded molecule movement is characterized by agar gel [5]. Carrageenan gel that can be used for magnetic resonance imaging (MRI) phantoms is formed with polysaccharides of seaweed. It is also flexible like phantoms produced with agar gel [6]. The polyvinyl alcohol (PVA) based tissue contains a PVA dissolved in water. It has more structural stability in a longer period than the other tissue-mimicking phantom methods [7]. On the other hand, the phantom models as commercial rigid plastics, polyurethane gel, gelatin-alginate, elastomeric (rubber-like) materials, and so on have been formed so far [1, 8, 9].

Since the purpose of the use of phantoms is usually calibration and testing, different imaging methods are used for their scanning. Dabrowski *et al.* presented a real vessel phantom and scanned it via projection radiography, CT, US, and MR [10]. Vogt *et al.* used MRI, CT, and ultrasound for imaging breast-mimicking tissue phantoms [11]. He *et al.* generated a breast phantom via three-dimensional (3D) printing and they used CT and MRI imaging modalities [12]. Nisar *et al.* presented a vascular phantom and compared their model obtained by carrying out CAD software to the CT scan [13].

The imaging of the above-mentioned different phantom samples with digital holography has a very important place in

terms of resolution and image quality. In addition, the displayed data can be stored in very small areas and reconstructed in three dimensions [14]. The quantitative phase image of the micro sized samples can be captured directly and reconstructed numerically with the digital holographic microscopy technique [15-18]. There have been several types of research employing digital holography microscopy to characterize the biological cells in the current literature. For example, Anand *et al.*, Rappaz *et al.*, FalckMiniotis *et al.* have used digital holography microscopy to fingerprint the red blood cells, tumor cellars, and fibroblasts, respectively [19-21]. In addition, in recent years, it is utilized to recover the images [22]. Although there are various researches in the literature about examining and recovering living cells using digital holography microscopy, the studies about using digital holography microscopy for phantoms are limited. In other respects, common methods such as filtered back projection, iterative reconstruction algorithms, etc. have been employed generally in phantom image reconstruction applications [23]. In this study, we imaged the created phantoms by means of the lateral shearing digital holography technique and performed the reconstruction process with a binary genetic algorithm.

The organization of this paper is as follows: Section II explains the binary genetic algorithm in detail. The preparation of the phantoms and the detailed expression of the optical imaging system is given in Section III. Experimental results are presented in Section IV. Finally, this paper is concluded in Section V.

## II. BINARY GENETIC ALGORITHM

The genetic reproduction, evaluation, and selection stages are the basis for GAs [24]. The population is initialized by the initialization step. The selection step enables the selection of the chromosomes that fit better for the formation of the mating pool. In this paper, a roulette wheel scheme is used [25]. The information shared between each pair of mating parents is performed by crossover schemes. The high value of probability is applied for crossover. The gene pairs are changed over a mutation operator and thus allow to obtain small variation for the fitness diversity in the population [26]. In this study, a binary mutation operator has been used for the simulations and the genes are produced randomly in the range of [0, 1]. The used algorithm for the binary mutation is detailed below,

**If random number < mutation probability**  
 ↓  
**Flip the gen bit value and assign it to chromosome**

In the last step, the fitness function is chosen to determine the error between the original and reconstructed images. Various measures can be used in this stage such as Root Mean Squared Error (RMSE), Mean Squared Error (MSE), and Mean Absolute Error (MAE) [27]. The GA operation can be terminated if the optimal solution is converged or the specified number of generations is reached. In this paper,

the MAE fitness function is used to reconstruct the image as defined in Eq. (1),

$$F = (1 + E_M)^{-1} \quad (1)$$

Here:  $E_M$  – is the MAE value between the reference and the computed reconstructions of BGA.

Since MAE is selected as the fitness function, the lower fitness function value means that the lowest difference between the reference and reconstructed one has the probability to be selected as parents for ensuing generations. In other words, the chromosomes that have lower misfits are preferred.

The steps of the BGA algorithm used in this study are presented in Algorithm 1.

---

### Algorithm 1

---

Initialize the population (M, N)  
 Evaluate the fitness function using Eq.(1)

**While** (end condition is not met) **do**  
     Select the chromosomes used by [20]  
     Crossover the parents and children  
     Perform the mutation operator  
     Evaluate the fitness function or a specified number of generations

Return the selection

---

where, M and N represent the numbers of chromosomes and genes, respectively.

In addition to selection, crossover, and mutation genetic operators, there have been some factors such as the size of the population, numbers of genes, bits, and generations, probabilities of crossover, and mutation which are set to make the algorithm work accurately. These parameters have a significant effect on the optimization performance of the algorithm. When the population size is large, the search area is explored more thoroughly with a longer computation time, while early convergence can be seen when the population size is very small. Also, the number of model parameters determines the number of genes. The increment in the number of parameters complicates the function by causing the model space size to be enlarged. Since the accuracy of the solution depends on the number of bits, the complexity and inappropriate values of the parameters make it difficult to explore the accurate solution. The crossover probability determines the new chromosomes to be obtained. Generally, a value between 0.8 and 0.95 is chosen as the crossover probability, since almost all parents are preferred to be replaced by their new chromosomes in the next generation. On the other hand, the mutation probability is often only 0.05% to 1% [28].

In this study, the population includes 100 individuals, and the probabilities of crossover and the mutation are constituted as 0.95 and 0.001, respectively. In addition, the crossover and mutation parameters are chosen as the same as the ones

presented in [24]. An example of these operators is given in Fig. 1.

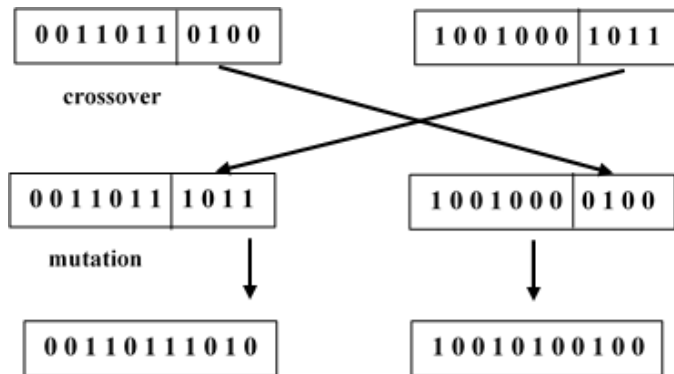


Fig.1. The crossover and mutation operators [25]

### III. PHANTOM GENERATION AND IMAGING SETUP

#### A. Preparation of Phantom Samples

The phantoms used in this study are generated with agar gel [14]. To mimic the human vascular system, grass and white balloon filled with water are used for the generated phantoms. The grasses and balloons are placed randomly in the generated phantoms as presented in Fig. 4a and Fig. 5a, respectively.

#### B. Lateral Shearing Digital Holographic Microscopy System

In this study, the produced phantom samples showing vascular structures are visualized with a lateral shearing digital holographic microscopy (LSDHM) system [29]. The configuration of LSDHM is shown in Fig. 2.

With the system presented in Fig. 2, a coherent light source is needed to record the information of the object to be imaged (in other words, to create an interference pattern). In this study, this requirement is supplied by means of a He-Ne laser with a wavelength of 632nm. For the beam emerging from the light source to proceed without scattering, a uniform Gaussian distribution is created by first passing it through a spatial filter. It is then collimated with the aid of a lens (100 mm focal length). After the collimated beam runs through the object, it is amplified with a microscopic objective (MO) so that it can be seen more clearly. The magnification of the MO used is 6X (NA=0.75). In addition, transparent phantom samples produced as objects are used.

As the magnified object is reflected on the front and back surfaces of the shearing plate, two sheared object beams are formed. The factor causing this shearing is the thickness of the shear plate used. In this study, a 6mm thick plane ruled reflection grating (PRRG) glass plate was used as the shearing plate. Finally, the hologram (interference pattern) is modeled by the use of two sheared object beams on the image sensor which is a CMOS camera.

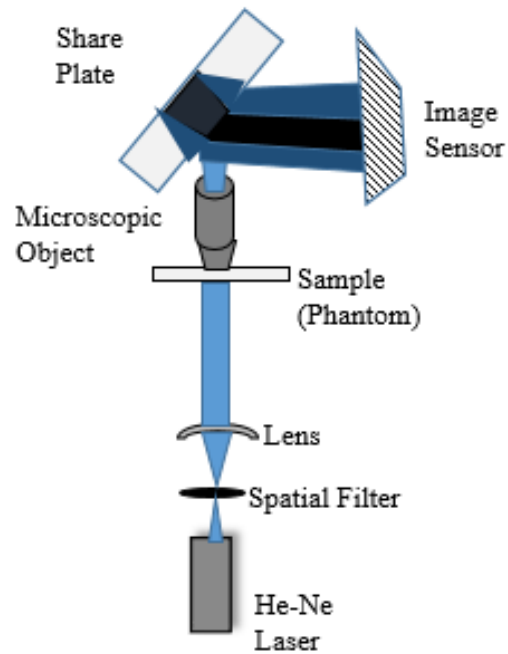


Fig. 2. The configuration of LSDHM

#### C. Field of View (FOV) and Resolution

Since the Field of View (FOV) is related to the visual angle of a lens, it affects the resolution and size of the captured image by the camera. If the measurement object moves away from the camera, the size of the region of the image increases. Accordingly, the captured individual pixels' mean resolution increase, too. That ensures the users see virtual content in enhanced veracity. Moreover, even though the angle of view is fixed, different sizes of FOV can be obtained when the lens is focused at different working distances. The full angle in terms of degrees related to the width of the sensor on which the lens will be used is defined as the angular field of view (AFOV) [30]. Therefore, AFOV is defined by the focal length of the lens as given in Eq. (2).

$$AFOV = 2 \tan^{-1} \left( \frac{H}{2f} \right) \quad (2)$$

Where:  $H$ –is the size of the sensor;  
 $f$ – is the focal length.

In addition, the relationship between the FOV and AFOV is defined in Eq. (3),

$$AFOV = 2 \tan^{-1} \left( \frac{FOV}{2xWD} \right) \quad (3)$$

Where:  $WD$ –is the working distance.

The sensor size relates to the X and Y pixels configuration. In this work, X and Y pixels are configured at 256x256. On the other hand, the focal length relates to the sensor size, the distance between the camera lens and object ( $WD$ ), and the

recorded object size ( $B$ ). The mathematical equation of focal length ( $f$ ) is given in Eq. (4).

$$f(mm) = \frac{WD}{1 + \frac{B}{0,0014x\sqrt{X^2 + Y^2}}} \quad (4)$$

In this study, the sensor size is calculated as 0.506 mm, when the X and Y pixels are configured a 256x256, and the  $WD$  is taken as 80 mm. In addition, the size of the recorded balloon and grass-made phantoms are 5 mm and 0.2 mm respectively. The used MO has 6X magnification with  $NA=0.75$ . For this reason, the size of phantoms is assumed to be 3mm and 1.2mm. In this context, the calculated values of focal lengths ( $f$ ) are 7.4mm and 23.75mm for the balloon and grass-made phantoms, respectively. Based on these ( $f$ ) values, the AFOV values are obtained as 3.92 mm and 1.22 mm, respectively. Moreover, the FOV values are calculated as 5.48 mm and 1.70 mm for the balloon and grass-made phantoms, respectively.

#### IV. RESULTS AND DISCUSSION

In this paper, two different phantoms are generated by using grass and a balloon to mimic the human vascular system. The simulations are conducted on MATLAB 2018b program to do the performance review of the binary genetic algorithm in digital holographic image reconstruction. The original images of generated phantoms are acquired with the help of the experimental setup given in Fig. 2. After the holograms of the original images are obtained, for the reconstruction of digital holographic images of the generated phantoms, the BGA algorithm given in Algorithm 1 is used and the original phantom images are tried to be obtained via BGA. The values of the BGA parameters of this study are presented in Table I. The algorithm has stopped when the determined maximum iteration number has been attained.

TABLE I  
THE USED QUANTITIES FOR BGA ALGORITHM

BGA Parameters	Determined values
Generations	5000
Probability crossover	0.95
Probability mutation	0.001
Elitism rate	20%

The originals, the binarized records, digital holographic, and BGA reconstructed phantom images are shown in Fig. 3 and Fig. 4 for the balloon and grass-made phantoms, respectively. The figures given with b and d in Fig. 3 and 4 correspond to the images of the recorded holograms and binarized reconstructed ones, respectively. The size of the original phantom images is 256x256. The best fit can be obtained by crossover and mutation operators with 5000 epochs and the reconstructed images have almost the same details as the original digital

holographic reconstructed ones as shown in Fig. 3 and Fig. 4. In addition, the fitness of the best elite graphs for the BGA can be seen in Fig. 3e and Fig. 4e with 5000 epochs.

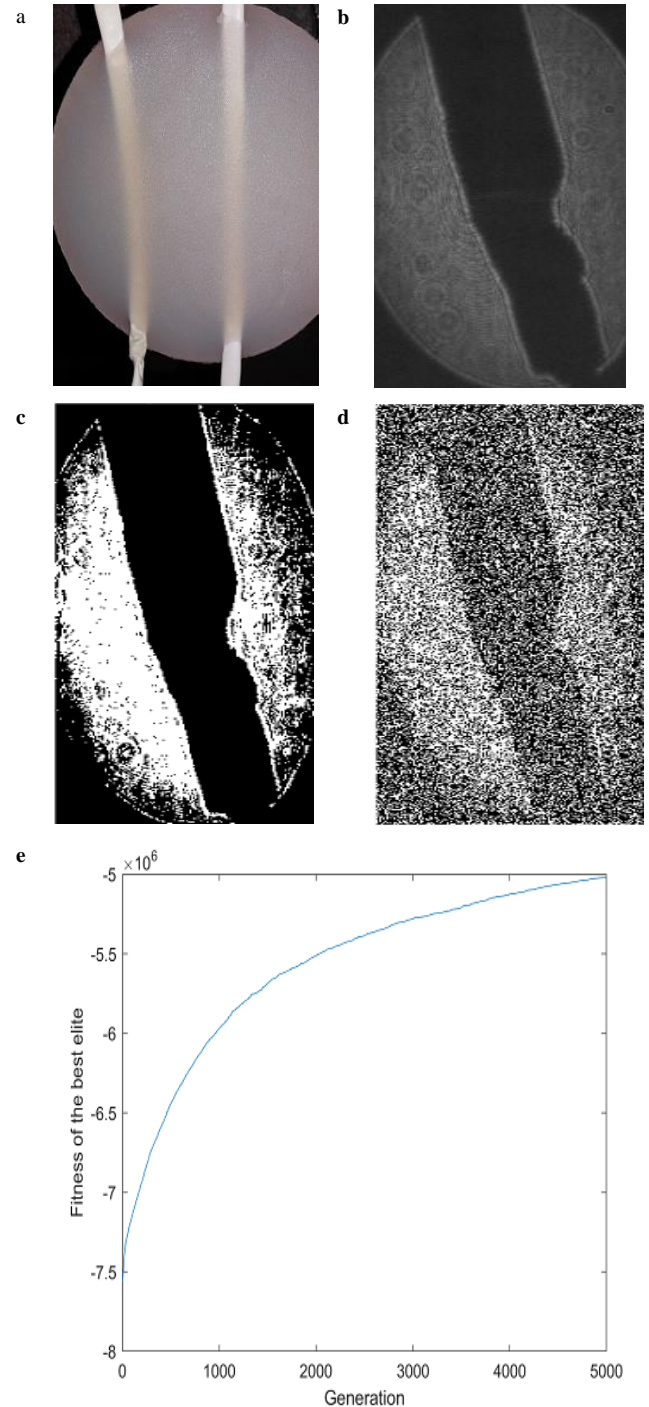


Fig. 3. Phantom with balloon a) Created phantom b) The image of recorded hologram c) Binarized recorded image d) Binarized reconstructed image e) Fitness graph

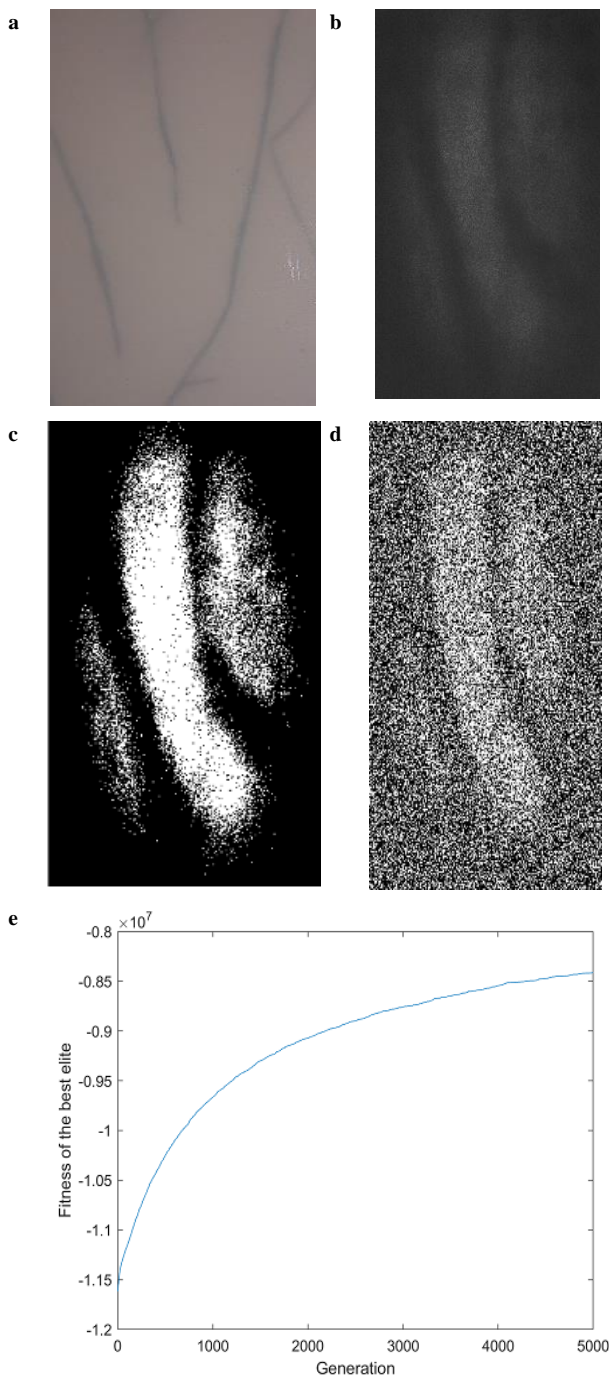


Fig. 4. Phantom with grass a) Created phantom b) The image of recorded hologram c) Binarized recorded image d) Binarized reconstructed image e) Fitness graph

In order to prove that the use of BGA for phantom image reconstruction in the LS-DHM system, our current study is compared with the existing applications in the literature given in Table II. For example, Günel and Kent propose a new approach, which utilizes genetic algorithms, to estimate a cross-sectional image by means of X-ray illumination for the reconstruction process. They also estimate the object parameters with some assumptions and the best results are obtained with the use of fuzzy genetic algorithms [31]. In this study, although the phantom image is reconstructed with GA

and FGA, the used phantom has not been obtained with a holographic system. However, in our proposed system, an artificial phantom is produced with a holographic system (LSDHM) that can be captured very small (in micro and nano-sized) objects, and a noise-free image can be obtained with the genetic algorithm. Uliana *et al.* investigated four methods such as the energy of the signal, integral of the modulus, peak-to-peak, and autocorrelation of the maximum value to estimate the PA signal amplitude. They aimed to form a thermal image by utilizing PA signal amplitude. The PA images of the tissue-mimicking phantom, which are fabricated with a gelatin/agar powder and submerged in a water tank, are used to perform the experiments. They notified that the usage of an evolutionary GA to optimize the parameters of thermal images is improved the error on average by 7.5% [32]. Although Uliana *et al.* obtained phantom images with PA, the system used is quite more complex than the LSDHM system. For this reason, the phantom acquisition is fatiguing. On the other hand, the usage of GA is for estimating the variations in PA signal amplitude, not for the reconstruction of the phantom image. Onur *et al.* proposed the use of the phase-shifting process within the Lateral shearing digital holographic microscopy. They aimed to increase the system stability, adjust the setup alignment and reduce the mechanical and unwanted vibrations. They also imaged the tissue-mimicking phantom manufactured using agar powder and distilled water [14]. Although Onur *et al.* used the LSDHM system for the production of mimicking phantoms for the first time, they used the phase-shifting technique for image reconstruction. However, this technique requires more than one image recording. To eliminate this problem and to reconstruct the images obtained with LSDHM in real-time, the usage of GA is proposed in our current work. Ziemczonok *et al.* performed a study that they visualized biological cell phantoms, which are formed with 3D-printed, via a holographic tomography microscope system. In the reconstruction process, the tomographic reconstruction algorithm is used. This algorithm bases on applying the Fourier diffraction theorem in the Rytov approximation [33]. Magliani *et al.* used genetic algorithms to find the diffusion parameters in several public image datasets. However, they obtained a better set of parameters and higher precision of the retrieval, GA is preferred for optimization not to for the reconstruction process. In addition, the phantom images are not imaged in their study [34]. Devi discussed the different medical imaging techniques by surveying the comprehensive survey. To evaluate the system, they also compared the soft computing methods based on a certain parameter. The performances of the fuzzy approach, machine learning, and genetic algorithm applications are investigated. Although the medical images are investigated, phantom images are not used in these methods [35]. Gouicem applied the Fuzzy penalty (FP) function for GA optimization in the field of image reconstruction. The real and synthetic image datasets are analyzed and these images are reconstructed from a few projections [36].

As mentioned above, there are many studies in the literature to obtain mimicking phantom images. However, in some of these studies, the stages of obtaining images are quite laborious. The systems used are quite complex. Therefore, there is a need

for optimization and parameter estimation using genetic algorithms.

TABLE II  
EXISTING STUDIES DEALING WITH RECONSTRUCTION  
TECHNIQUES AND PHANTOM IMAGES

Authors	Purpose	Techniques/Methods	Material
Günel and Kent (1998)[31]	To determine the object parameters and to estimate a cross-sectional image from an objects' X-Ray projections.	Reconstruction with genetic and fuzzy genetic algorithms	Head phantom
Uliana <i>et al.</i> (2018)[32]	To form a thermal image by estimating the variations in PA signal amplitude.	Imaging with Photoacoustic (PA)	A tissue-mimicking phantom fabricated using a gelatin and agar powder
Onur <i>et al.</i> (2021) [14]	To image the soft tissue-mimicking phantom for early diagnosis	Phase shifted-lateral shearing digital holographic microscopy	Soft tissue-mimicking phantoms
Ziemczonok <i>et al.</i> (2019)[33]	To visualize the 3D-printed biological cell phantoms by means of a Holographic tomography system	Tomographic reconstruction algorithm	3D-printed biological cell phantoms
Magliani <i>et al.</i> (2019)[34]	To optimize the Diffusion Parameters via genetic algorithms	Not defined	Public image datasets
Devi <i>et al.</i> (2021)[35]	To discuss the various biomedical imaging techniques with a comprehensive survey	Fuzzy logic, artificial neural network, genetic algorithm, machine learning	Several medical images
Gouicem <i>et al.</i> (2012)[36]	To reconstruct the computed tomography image by using the Fuzzy and GA optimization	Image Reconstruction GA, fuzzy inference	Computer Tomography (CT) image (real and synthetic image)

In addition, in some studies, genetic algorithm has been used for image recovery. However, the materials used in these

studies are synthetic data. In order to eliminate these problems, the phantoms are produced with the lateral shearing digital holography technique, which allows the imaging of micro and nano-sized particles. In addition, the usage of a genetic algorithm for the real-time reconstruction of images obtained from LSDHM has been suggested. To the best of the authors' knowledge, the experimentally produced phantoms have not been imaged with an optical system and recovered by a genetic algorithm. Thus, both the non-contact imaging of the vascular mimicking phantom images obtained with a holographic system and the recovery of these images in real-time with the genetic algorithm is provided.

## V. CONCLUSIONS

In this paper, we presented the task of using digital holography and binarized genetic algorithm for imaging tissue-mimicking phantoms. The two different structured phantoms made of grass and balloon that are mimicking the human vascular system are evaluated for the experiments. The necessity of phantom usage arises from providing a more realistic imaging environment and ensuring that all kinds of operations are performed without the need for real tissue. Therefore, it is a medically important task to generate either different tissue mimicking structures or visualize or reconstruct them with higher quality. The results obtained from this study have shown that optimal solution can be obtained by using BGA and image reconstruction can be achieved using BGA as well as digital holography.

## REFERENCES

- [1] P. Pasyar, S. Masjoodi, Z. Montazeriani, and B. Makkiabadi, "A digital viscoelastic liver phantom for investigation of elastographic measurements." *Computers in Biology and Medicine*, vol. 127, 2020, pp. 104078.
- [2] R. A. O. Jaime, R. H. Q. Basto, B. Lamien, H. R. B., Orlande, S., Eibner, and O. Fudym, "Fabrication methods of phantoms simulating optical and thermal properties." *Procedia Engineering*, vol. 59, 2013, pp. 30 – 36.
- [3] K. A. Abdullah, M. F. McEntee, W. Reed, and P. L. Kench, "Development of an organ specific insert phantom generated using a 3D printer for investigations of cardiac computed tomography protocols." *Journal of Medical Radiation Science*, vol. 65, no. 3, 2018, pp. 175-183.
- [4] S. Singh, and R. Repaka, "Numerical study to establish relationship between coagulation volume and target tip temperature during temperature-controlled radiofrequency ablation." *Electromagnetic Biology and Medicine*, vol. 37, 2018, pp. 13-22.
- [5] T. Kondo, M. Kitatuji, Y. Shikinami, K. Tuta, and H. Kanda, "New tissue mimicking materials for ultrasound phantoms." In *Proceedings of IEEE Ultrasonic Symposium*, vol. 3, 2005, pp. 1664-177.
- [6] E. In, H. Naguib, and M. Haider, "Mechanical stability analysis of carrageenan-based polymer gel for magnetic resonance imaging liver phantom with lesion particles." *Journal of Medical Imaging*, vol. 1, no. 3, 2014, pp. 035502.
- [7] M. Arif, A. Moelker, and T. van Walsum, "Needle tip visibility in 3D ultrasound images." *Cardio Vascular and Interventional Radiology*, vol. 41, 2018, pp. 145-152.
- [8] M. Kavitha, M. Ramasubba Reddy, and S. Suresh, "Modelling, design and development of tissue mimicking phantoms for ultrasound elastography." 2012 IEEE-EMBS Conference on Biomedical Engineering and Sciences, 2012, pp. 564-567.
- [9] Y. H. Kao, O. S. Luddington, S. R. Culleton, R. J. Francis, and J. A. Boucek, "A gelatin liver phantom of suspended 90Y resin microspheres to simulate the physiologic microsphere biodistribution of a

- postradioembolization liver." *Journal of Nuclear Medicine Technology*, vol. 42, no. 4, 2014, pp. 265-273.
- [10] W. Dabrowski, J. Dunmore-Buyze, R.N. Rankin, D.W. Holdsworth, and A. Fenster, "A real vessel phantom for imaging experimentation." *Medical Physics*, vol. 24, no. 5, 1997, pp. 687-693.
- [11] W.C. Vogt, C. Jia, K.A. Wear, B.S. Garra, and T.J. Pfefer, "Phantom-based image quality test methods for photoacoustic imaging systems." *Journal of Biomedical Optics*, vol. 22, no. 9, 2017, pp.095002-1-14.
- [12] Y. He, Y. Liu, B.A. Dyer, J.M. Boone, S. Liu, T. Chen, F. Zheng, Y. Zhu, Y. Sun, Y. Rong, and J. Qui, "3D-printed breast phantom for multi-purpose and multi-modality imaging." *Quantitative Imaging In Medicine And Surgery*, vol. 9, no. 1, 2019.
- [13] H. Nisar, J. Moore, R. Piazza, E. Maneas, E.C.S. Chen, and T.M. Peters, "A simple, realistic walled phantom for intravascular and intracardiac applications." *International Journal of Computer Assisted Radiology and Surgery*, vol. 15, 2020, pp. 1513-1523.
- [14] T.O., Onur, G. Ustabas Kaya, and C. Kaya, "Phase shifted-lateral shearing digital holographic microscopy imaging for early diagnosis of cysts in soft tissue-mimicking phantom." *Applied Physics B*, vol. 127, no. 61, 2021.
- [15] A. Anand, P. Vora, S. Mahajan, V. Trivedi, V. Chhaniwal, A. Singh, L. Leitgeb, and B. Javidi, "Compact, common path quantitative phase microscopic techniques for imaging cell dynamics." *Pramana*, vol.82, no. 1, 2014, pp. 71-78.
- [16] A. S. G. Singh, A. Anand, R. A. Leitgeb, and B. Javidi, "Lateral shearing digital holographic imaging of small biological specimens." *Optics Express*, vol. 20, 2012, pp. 23617-23622.
- [17] Y. Park, C. Depeursinge, and G. Popescu, "Quantitative phase imaging in biomedicine." *Nature Photonics*, vol. 12, no. 10, 2018, pp. 578-589.
- [18] S. Devinder, A. Lal, T. R. Dastidar, and S. K. Dubey, "Quantitative analysis of numerically focused red blood cells using subdivided two-beam interference (STBI) based lateral-shearing digital holographic." *arXiv:1909.03454 [eess.IV]*, 2019.
- [19] A. Anand, V. K.Chhaniwal, N. R.Patel, and B. Javidi, "Automatic identification of malaria-infected RBC with digital holographic microscopy using correlation algorithms." *IEEE Photonics Journal*, vol. 4, no. 5, 2012, pp. 1456-1464.
- [20] B. Rappaz, B. Breton, E. Shaffer, and G. Turcatti, "Digital holographic microscopy: a quantitative label-free microscopy technique for phenotypic screening." *Combinatorial Chemistry & High Throughput Screening*, vol. 17, no. 1, 2014, pp. 80-88.
- [21] M. Falck Miniotis, A. Mukwaya, and A. Gjørloff Wingren, "Digital holographic microscopy for non-invasive monitoring of cell cycle arrest in L929 cells." *PLoS One*, vol.9, no. 9, 2014, pp. e106546.
- [22] X. Quan, O. Matoba, and Y. Awatsuji, "Image recovery from defocused 2D fluorescent images in multimodal digital holographic microscopy." *Optics Letters*, vol. 42, 2017, pp. 1796-1799.
- [23] N. Miyaji, K. Miwa, A. Tokiwa, H. Ichikawa, T. Terauchi, M. Koizumi, and M. Onoguchi, "Phantom and clinical evaluation of bone SPECT/CT image reconstruction with xSPECT algorithm." *European Journal of Nuclear Medicine and Molecular Imaging*, vol. 10, no.71, 2020, pp. 2-12.
- [24] D. E. Goldberg, *Genetic Algorithms in Search, Optimization and Machine Learning*, AddisonWesley, Reading Massachusetts, 1989.
- [25] M. Mitchell, *An Introduction to Genetic Algorithms*, MIT Press, Cambridge, Massachusetts, 1999.
- [26] A. Hussain, and Y. S. Muhammad, "Trade-off between exploration and exploitation with genetic algorithm using a novel selection operator." *Complex & Intelligent Systems*, vol. 6, 2020, pp. 1-14.
- [27] M. K. Ahamad, "Comparative analysis the fitness function of k-means and kernel fisher's discriminant analysis (KFDA) with genetic algorithm." *European Journal of Molecular & Clinical Medicine*, vol. 7, no. 11, 2020, pp. 6231-6241.
- [28] A. Hassanat, K. Almohammadi, E. Alkafaween, E. Abunawas, A. Hammouri, and V. B. S. Prasath, "Choosing mutation and crossover ratios for genetic algorithms- a review with a new dynamic approach." *Information*, vol. 10, no. 390, 2019, pp. 2-36.
- [29] G. Ustabas Kaya, "Imaging of transparent objects with phase shifting-lateral shearing digital holographic microscopy." *IEEE, 2020 28<sup>th</sup> Signal Processing and Communications Applications Conference (SIU)*, 2020.
- [30] J.E. Greivenkamp, *Field Guide to Geometrical Optics*, SPIE Press, Bellingham, WA, 2004.
- [31] T. Günel, and S. Kent, "Genetic approach for the determination of object parameters from X Ray projections." *Turkish Journal of Electrical Engineering and Computer Science*, vol.6, no.3, 1998, pp. 277-286.
- [32] J. H. Uliana, D. R. T. Sampaio, A. A. O. Carneiro, and T. Z. Pavan, "Photoacoustic-based thermal image formation and optimization using an evolutionary genetic algorithm." *Biomed Research International*, vol. 34, no. 2, 2018, pp. 147-156.
- [33] M. Ziemczonok, A. Kuś, P. Wasylczyk, and M. Kujawińska, "3D-printed biological cell phantom for testing 3D quantitative phase imaging systems." *Scientific Reports*, vol. 9, no. 1, 2019, pp. 1-9.
- [34] F. Magliani, L. Sani, S. Cagnoni, and A. Prati, "Genetic algorithms for the optimization of diffusion parameters in content-based image retrieval." *arXiv:1908.06896v1 [cs.CV]* 19 Aug 2019.
- [35] M. Devi, S. Singh, S. Tiwari, S. C. Patel, and M. T. A. Ayana, "Survey of soft computing approaches in biomedical imaging." *Journal of Healthcare Engineering*, vol. 2021, 2021, pp. 1-15.
- [36] A. M. T. Gouicem, K. Benmahammed, R. Draï, M. Yahi, and A. Taleb-ahmed, "Multi-objective GA optimization of fuzzy penalty for image reconstruction from projections in X-ray tomography." *Digital Signal Processing*, vol. 22, no. 3, 2012, pp. 486-496.

## BIOGRAPHIES



**TUĞBA ÖZGE ONUR** is an Assistant Professor in the department of Electrical Electronics Engineering at Zonguldak Bülent Ecevit University. She received her MSc and PhD degrees, with highest honors, in Electrical-Electronics Engineering from Zonguldak Bülent Ecevit University in 2008 and 2016, respectively. Her doctoral thesis study was partly carried out at Luleå University of Technology (Luleå, Sweden) and University of Wisconsin-Madison (Madison, Wisconsin, USA). Her research interests include signal and image processing, ultrasound signal processing, system identification and nonlinear systems. She has published papers in the field of signal processing applications.



**GÜLHAN USTABAŞ KAYA** is a Research Assistant Dr. in the department of Electrical-Electronics Engineering at Zonguldak Bülent Ecevit University. She received her MSc and PhD degrees in Electrical-Electronics Engineering from Zonguldak Bülent Ecevit University in 2013 and 2019, respectively. Her interest fields are in the development of novel techniques and applications in digital holography, interferometry, microscopy, photonics, signal and image processing, data mining and machine learning. She has published papers in the field of optics, signal processing and machine learning applications. She is also an OSA member.